Lasers in Surgery and Medicine 25:407–413 (1999)

Laser–Tissue Interaction With a High-Power 2-μm Fiber Laser: Preliminary Studies With Soft Tissue

Mark C. Pierce, BSc,* Stuart D. Jackson, PhD, Mark R. Dickinson, PhD, and Terence A. King, PhD

Laser Photonics Research Group, Department of Physics and Astronomy, University of Manchester, Manchester M13 9PL, United Kingdom

Background and Objective: **Recent developments in fiber laser technology have introduced highly efficient, compact sources with high output beam quality. The first laser–tissue interaction studies with a high-power 2-μm fiber laser were conducted.**
Study Design/Materials and Methods: **Chicken breast and porcine muscle tissue samples were subjected to continuous wave (cw) irradiation at 800-mW and 5-W output power levels, with spot sizes of approximately 150 μm. After laser irradiation, samples were inspected with an optical microscope and prepared for histologic processing.**
Results: **Evaluation of surface changes in tissue samples indicated an interaction similar in nature to those previously demonstrated with other cw lasers, but with photothermal ablation characteristics typical of strongly absorbed lasers operating in the infrared wavelength region. An ablation velocity of 0.27 mm·sec^{-1} in porcine tissue was determined at 800-mW incident power. Histopathologic analysis demonstrated the formation of lesions with minimal damage at boundaries and no evidence of carbonization.**
Conclusions: **Results indicate that this fiber laser has the potential to fulfill applications in the medical field. Lasers Surg. Med. 25:407–413, 1999.**

Key words: continuous wave; laser ablation; laser surgery; mid-infrared; thermal effects

INTRODUCTION

Lasers operating at wavelengths in the mid-infrared region have become increasingly popular in recent years as alternatives to mechanical drills and scalpels in areas of surgery and medicine. Precise, efficient ablation of hard and soft biological material is made possible by the strong coupling of optical energy to tissue. Water is the primary absorbing component in tissue at wavelengths above ~1.4 μm, with absorption increasing through the mid-infrared to a maximum at approximately 3 μm [1]. Absorption of laser energy results primarily in thermally induced effects taking place as tissue temperature rises. Protein denaturation takes place at 60–70°C, water vaporizes at ~100°C, and tissue carbonization occurs at higher temperatures. Operating near the OH absorption band, around 1.9 μm, suggests the potential for an interaction characterized by accurate tissue removal, accompanied by thermally induced coagulative and haemostatic effects.

At present, numerous applications could benefit from a laser source offering precise ablation with coagulation of superficial tissue including neurosurgery, tumor resection, cardiology, ophthalmology, and general surgery [2,3].

Contract grant sponsors: Engineering and Physical Sciences Research Council, Department of Trade and Industry Link, Photonics Initiative Solid State Lasers for Applications in Medicine.

*Correspondence to: Mark C. Pierce, Laser Photonics Research Group, Department of Physics and Astronomy, University of Manchester, Manchester M13 9PL, UK.
E-mail: mp@fs4.ph.man.ac.uk

Accepted 2 August 1999

The development of fiber laser technology has introduced highly efficient and compact sources potentially well suited to the clinical environment. Near–diffraction–limited output beam quality allows a more tightly focused beam to be formed than with multimode laser output, potentially enabling procedures to be carried out with increased precision. These lasers may be made to operate in continuous wave (cw) or pulsed mode, with recently reported output powers of >35 W at a wavelength of 1.1 μm [4]. This study describes the findings of preliminary experiments investigating the interaction between a Tm–doped silica fiber laser and soft biological tissues. Features of the laser–tissue interaction are highlighted and described, accompanied by microscopic images of surfaces and histologic sections of craters and slots cut in tissue.

MATERIALS AND METHODS

The laser used in the present study is a recently developed diode-cladding-pumped Tm-doped silica fiber laser with an operating wavelength of 1.880–2.033 μm by adjusting the fiber length and output mirror reflectivity. The double-clad fiber has a 17-μm-diameter core and a numerical aperture of 0.2 and was fabricated at the Optoelectronics Research Centre (University of Southampton, UK). The pump source is a specially designed diode laser unit (Diomed Ltd., Cambridge, UK), providing 25 W of total output power at the 790-nm pump wavelength, enabling >5 W of fiber laser power to be obtained in cw mode. Details of the fiber laser design and operation have been reported elsewhere [5]. All experiments described in the present study were performed at a wavelength of 1.98 μm.

The specimens used were porcine muscle tissue and chicken breast, obtained on the day of experiment and refrigerated until 1 hour before the experiment, when the tissue was allowed to reach room temperature. Samples were mounted on an x–y–z translation stage and irradiated in air. The fiber laser output was focused onto the tissue surface by single CaF_2 lenses with focal lengths of 25–75 mm. Holes were made by exposing the surfaces of stationary tissue samples positioned at the focus of the incident laser beam. Slots were made by translating tissue samples across the focus of the beam at a constant speed, for single or multiple passes. The remaining unabsorbed visible pump light emerging from the pump cladding (~200 mW) assisted in targeting and alignment, and the laser power was monitored regularly with a Coherent 210 power meter.

Tissue specimens were inspected under an optical microscope immediately after irradiation to evaluate surface changes, and specimens were stored in 10% neutral buffered formalin for histologic processing. Samples were routinely processed, fixed in paraffin wax, sectioned, and stained with hematoxylin and eosin, thereby enabling the nature and extent of damage in holes and slots to be assessed. The ablation velocity in tissue was determined by measuring the time taken for the laser beam to perforate tissue samples of measured thickness. The point of perforation was detected by placing a power meter behind the tissue sample. Multiple sites were targeted in a number of tissue samples, resulting in more than 100 lesions being evaluated.

RESULTS

Stationary Tissue Samples

The fiber laser–tissue interaction was characterized by three distinct stages, as described previously for interactions with other cw lasers [6–8]. Photomicrographs of chicken breast tissue sample surfaces on irradiation with 800 mW from the fiber laser at 1.98 μm are presented in Figure 1 for a range of exposure times, illustrating the evolution of the ablation process. The spot size was estimated to be ~150 μm in diameter, resulting in an incident irradiance of approximately 100 $W \cdot mm^{-2}$. In the first stage, a region of dehydrated tissue instantaneously formed, which rapidly propagated both radially outward and into the tissue from the irradiated site. The arrows in Figure 1A indicate the range of the thermally affected zone 0.5 seconds after initial exposure. The second stage followed at ~5 seconds, with water vaporization and bubbling observed at the tissue surface, accompanied by a popping and crackling sound and visible tissue rupture. The arrow in Figure 1B indicates expanding pockets of water and vapor near the tissue surface. The ablation front was seen to advance into the tissue with continued irradiation of a single site. The third stage of the interaction process began at approximately 10 seconds, with the first signs of tissue browning, which became progressively darker until a black char formed around the edge of the ablation crater (Fig. 1C). This charred region increased in size to 100–150 μm in width with prolonged irradiation as the tissue surface became increasingly dehydrated. With irradiation at 5 W,

Fig. 1. Surface photomicrographs of chicken breast samples at a range of exposure times during irradiation with a fiber laser output of 1.98 μm at 800 mW. **A:** After an initial exposure of 0.5 seconds, a thermally affected zone, indicated by arrows, was formed, growing in size with exposure time. **B:** After 5.1 seconds, expanding pockets of water and vapor are visible near the surface, as shown by the arrow. **C:** After 17.0 seconds, following the stages of char formation beginning with initial browning, carbonized tissue formed around the edge of the ablation crater.

the ablation process appeared to proceed through the same series of stages but at a faster rate. At the 5-W power level, tissue removal was initiated within 1 second of exposure to the laser, followed by onset of carbonization at ~3 seconds.

The diameter of the visibly affected surface zone in chicken breast tissue is shown in Figure 2 as a function of laser exposure time. Data points shown represent mean diameters following inspection under an optical microscope, immediately after irradiation at 800 mW. The affected zone was defined as that region which had undergone visible whitening (Fig. 1A).

Figure 3 presents the time taken for the laser beam to penetrate through porcine tissue samples of measured thickness at an incident power level of 800 mW. Most tissue samples were 1.5–3.5 mm thick, and a linear fit to all data points (A in Fig. 3) produced an ablation velocity of 0.04 mm·sec^{-1} (correlation coefficient r = 0.90, $P < 0.0001$, n = 54). In practice, as the ablation front moves forward into the tissue, the irradiance decreases as a consequence of the increasing incident spot size as the sample surface moves beyond the beam focus. Ideally, tissue samples would be thin in comparison with the depth of focus of the laser beam, but the difficulty in preparing and measuring samples thinner than ~1.5 mm resulted in a lack of data points in this region. However, by plotting a linear fit to only those points representing the thinnest samples (B in Fig. 3) and including a point at the origin, a value for the ablation velocity of 0.27 mm·sec^{-1} (r = 0.97, $P < 0.001$, n = 7) was obtained.

Tissue samples irradiated under a range of conditions were processed for histologic analysis. Structural alterations of cells and collagen provide an indication of the range and extent of thermally induced effects. Figure 4 shows a section of

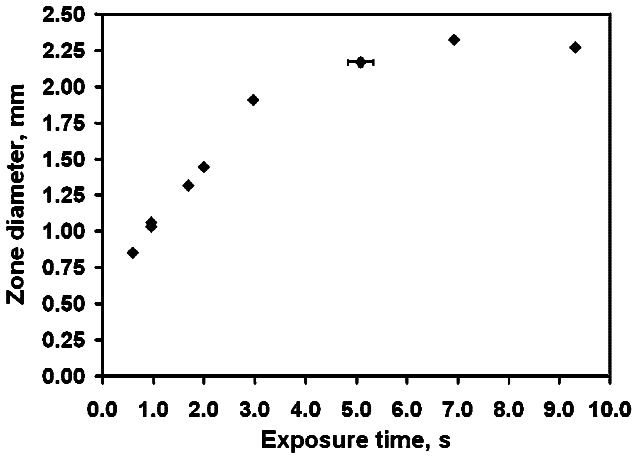

Fig. 2. Diameter of the visibly effected surface zone in porcine samples during 10 seconds of fiber laser irradiation at 800 mW.

a hole formed in porcine muscle tissue after 12 seconds of laser exposure at 5 W. The hole is approximately 1.5 mm in diameter at the sample surface and 3.3 mm in depth. Normal muscle tissue is seen to define the boundary of the hole, with remnants of vacuolated tissue in evidence, consistent with a zone of tissue reaching temperatures close to 100°C during the ablation process. Some dark charring is present at the surface, a feature typical of lesions formed by extended exposure times (>10 seconds at this power level). Figure 5 shows a cross section of a hole made by 0.5 sec of laser exposure at 5 W. Vacuolated tissue is present in the crater, but there are no signs of char formation or carbonization. There also appears to be an approximately 200-μm-wide region of coagulated tissue around the periphery of the hole, indicated by more densely packed muscle fibers, characteristic of water-dominated thermal tissue effects taking place during laser irradiation [9].

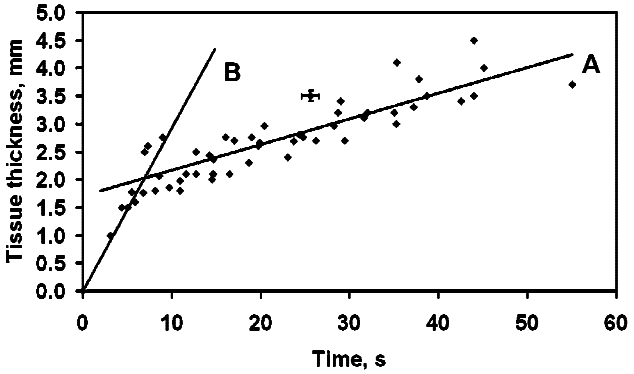

Fig. 3. Time taken for the fiber laser to penetrate porcine tissue samples of measured thickness, at an incident fiber laser power of 800 mW. **A:** Linear fit to all data points. **B:** Linear fit to data points representing the thinnest samples only, indicating a minimum cut rate of 0.27 mm·sec^{-1}.

Moving Tissue Samples

Surface photomicrographs of slots cut in chicken breast tissue at an incident power of 800 mW are shown in Figure 6. Translating the tissue across the focus of the laser beam at 0.25 mm·sec^{-1} resulted in carbonization along the walls and base of the slot (Fig. 6A). Open arrows define the range of char formation, and closed arrows indicate the extent of thermally affected tissue. By moving the tissue at 25 mm·sec^{-1}, prolonged exposure of any one point is avoided, resulting in a clean cut, with no observed carbonization or char formation (Fig. 6B).

Figure 7 shows a longitudinal section across the edge of a slot cut in porcine tissue, formed by traversing the sample across the focus of the laser beam at 0.25 mm·sec^{-1}, enabling three zones of damage to be identified. Region A containing dark stained tissue on the right-hand side indicates normal muscle tissue, region B in the center indicates vacuolated tissue, and the region to the left indicated by the arrow demonstrates the onset of charring at the crater edge. Reducing the exposure duration, in this case cutting a slot by traversing the tissue sample across the focus of the beam at ~25 mm·sec^{-1}, produced a clean boundary with normal tissue at the margins and no sign of carbonization (Fig. 8). This suggests making rapid multiple passes when cutting slots in tissue rather than making a slow single pass with extended exposure at any given point. An interesting effect was observed in a few of the histologic specimens. Basophilic collageneous septa were seen to extend laterally into the muscle, indicated by particularly dark histologic staining. Collageneous proteins swell in response to heat [9], indicating the conduction of thermal energy away from the target site.

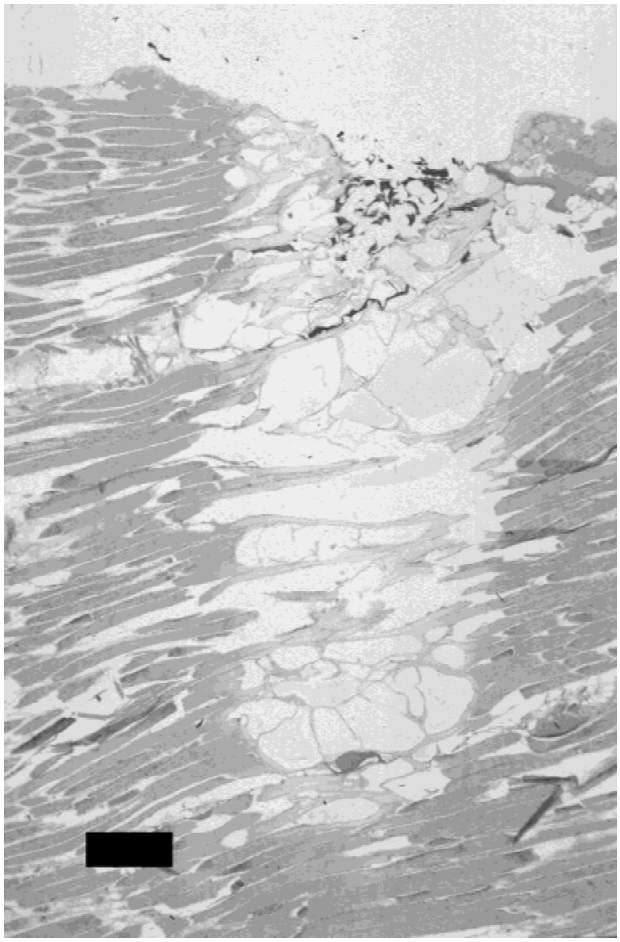

Fig. 4. Section of a hole formed in porcine muscle tissue after 12 seconds of fiber laser exposure at 5 W. Remnants of vacuolated tissue are evident in the crater, with a region of carbonized tissue at the surface. Scale bar = 500 μm.

DISCUSSION

Preliminary tissue interaction studies with a Tm-doped silica fiber laser have been performed with the intention of evaluating the potential of the laser for use in medical applications. Fiber laser technology is an emerging source of laser light, with characteristics making it well-suited to the needs of medical personnel. The laser used in the present study provided >5 W of output power in the 2-μm-wavelength region with high output beam quality and has the inherent potential for fiber delivery. The generation of potentially damaging stress waves in tissue, a factor often asso-

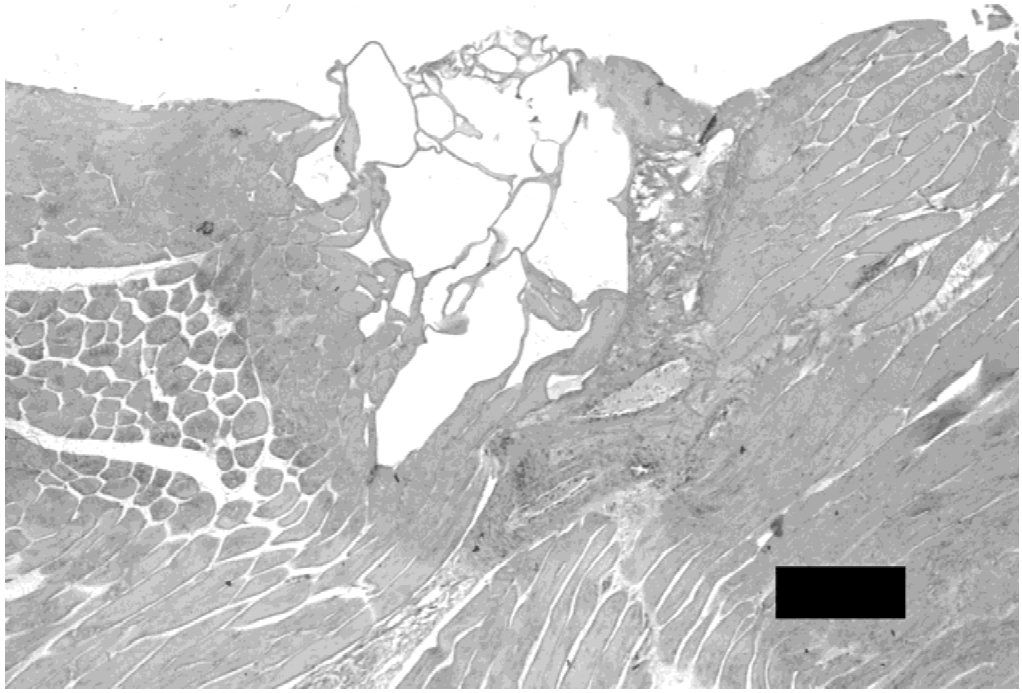

Fig. 5. Section of a hole made in chicken breast tissue by 0.5 seconds of fiber laser exposure at 5 W. Vacuolated tissue is present in the crater, but there are no signs of char formation or carbonization. Scale bar = 250 μm.

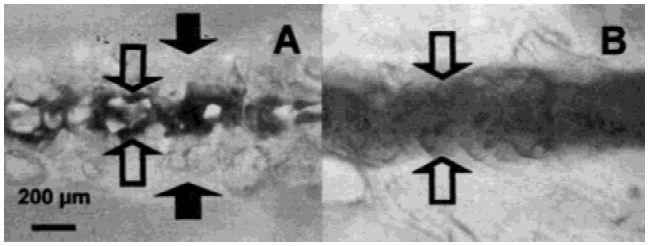

Fig. 6. Surface photomicrographs of slots cut in chicken breast tissue at 800-mW incident fiber laser power. **A:** Char formation was evident in the slot when the sample was translated across the laser beam at 0.25 mm·sec^{-1}. Open arrows indicate the range of charring, and closed arrows indicate the total range of observed thermal effects. **B:** Translating the tissue surface across the beam at 25 mm·sec^{-1} produced a clean slot without charring; arrows indicate the range of the slot.

ciated with pulsed systems, is avoided by use of the cw mode [10].

Figure 2 shows the diameter of the surface zone visibly affected by laser irradiation as a function of laser exposure time. This gives an indication of the lateral range of thermal effects in irradiated tissue. The size of the zone grows more rapidly during the first stage of ablation because energy is deposited primarily close to the tissue surface. As water is removed from the tissue, local thermal conductivity decreases, resulting in reduced heat conduction to the surrounding area. Once the tissue surface is broken and the ablation front advances into the tissue, absorption increases in the darker, charred crater edge, also resulting in reduced propagation of thermal energy to the edge of the dehydrated zone.

The cut rate in tissue was determined by recording the time taken for the laser to penetrate samples of measured thickness. As holes were made in samples, the interaction surface moved into the tissue, away from the beam focus, resulting in an increased spot size and reduced irradiance. Effects of absorption in crater walls and scattering from ejected debris will also contribute to reducing incident irradiance at depths in tissue. A linear fit to all data (Fig. 3) therefore represents an underestimate of the ablation velocity, whereas considering ablation over only the first 1.5 mm into tissue provides a more accurate value for the ablation velocity when the interaction surface is maintained at the beam focus. By including a data point at the origin in the linear fit, the revised value obtained for the ablation velocity represents a lower limit because in reality tissue ablation is initiated after a finite delay from the onset of irradiation.

Mechanisms of tissue removal on irradiation with cw sources have been described by others [6,7], with specific interaction pathways depend-

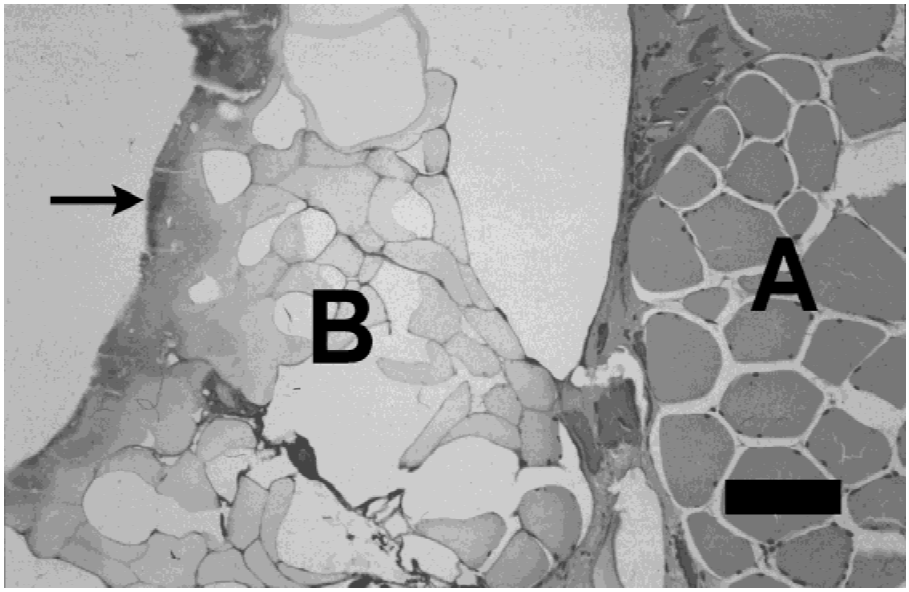

Fig. 7. Section across the edge of a slot cut in porcine tissue at 5 W fiber laser exposure, translating the sample across the focus of the beam at 0.25 mm·sec^{-1}. Region **A** containing dark stained tissue on the right-hand side indicates normal muscle tissue; region **B** in the center indicates vacuolated tissue; and the region to the left demonstrates the onset of charring at the crater edge, indicated by the arrow. Scale bar = 75 μm.

ing on particular laser and tissue parameters. Explosive ablation in aortic and myocardial bovine tissues with cw Nd:YAG and argon ion lasers has been described as a three-phase process characterized by tissue removal through explosive vaporization or "popcorn" and cyclic carbonization [7]. Soft tissue removal with the CO_2 laser proceeds by the rapid heating of tissue water to above 100°C, forming expanding, high-pressure vapor pockets. Once the tensile strength of the surrounding tissue is exceeded, debris and vapor are forcibly ejected from the surface [11]. Although tissue optical properties differ greatly over the range of wavelengths discussed in the present study, some insight into the nature of the 2-μm fiber laser–tissue interaction can be drawn based simply on tissue absorption. The primary distinction between these two interactions, with the deeply penetrating Nd:YAG/argon ion lasers and the strongly absorbed CO_2 laser, is the degree to which laser energy is transferred to tissue in each case. Absorption coefficients for CO_2 laser-irradiated tissues are several times higher than those for Nd:YAG or argon ion laser-irradiated tissues due mainly to the particularly strong absorption of infrared wavelengths by water. Consequently, at 10.6 μm, the interaction takes place more rapidly and much nearer to the tissue surface than that with the more penetrating 1,064-nm and 488/514-nm wavelengths of the Nd:YAG and argon ion lasers, respectively. Although typically an order of magnitude lower than at the CO_2 wavelength, tissue absorption coefficients in the 2-μm wavelength region are still significantly higher than at near-infrared and visible wavelengths. This factor suggests a photothermal mechanism of interaction similar to that described for the CO_2 laser, but with accompanying features consistent with cw tissue ablation in general. The three-phase process characteristic of the cw interaction was clearly observed at the tissue surface, but with particularly rapid onset of the "popcorn" effect, a consequence of the strong coupling of energy to tissue at this wavelength. Ablation with less strongly absorbed lasers may only proceed after tissue browning or the formation of a charred layer to enhance absorption, with subsequent tissue removal following a cyclic vaporization and recarbonization process. Histology showed three zones of damage, consistent with the model by McKenzie [11] for CO_2-irradiated soft tissue. However, it was found that at 5 W incident power, by limiting exposure times to <3 seconds or traversing samples across the focus of the laser beam at 25 mm·sec^{-1}, holes and slots were formed with minimal damage and no signs of carbonization at the boundaries. In general, carbonization may be prevented by limiting the incident irradiance. The degree to which energy is absorbed in tissue at the 2-μm wavelength enables ablation to occur through explosive water vaporization, before the onset of carbonization or char formation. This "clean" method of tissue removal is crucial to subsequent tissue healing and regeneration processes at the boundaries of holes, slots, and bulk excisions. Samples processed for histology demonstrate the ability of the laser to make clean incisions in tissue without producing

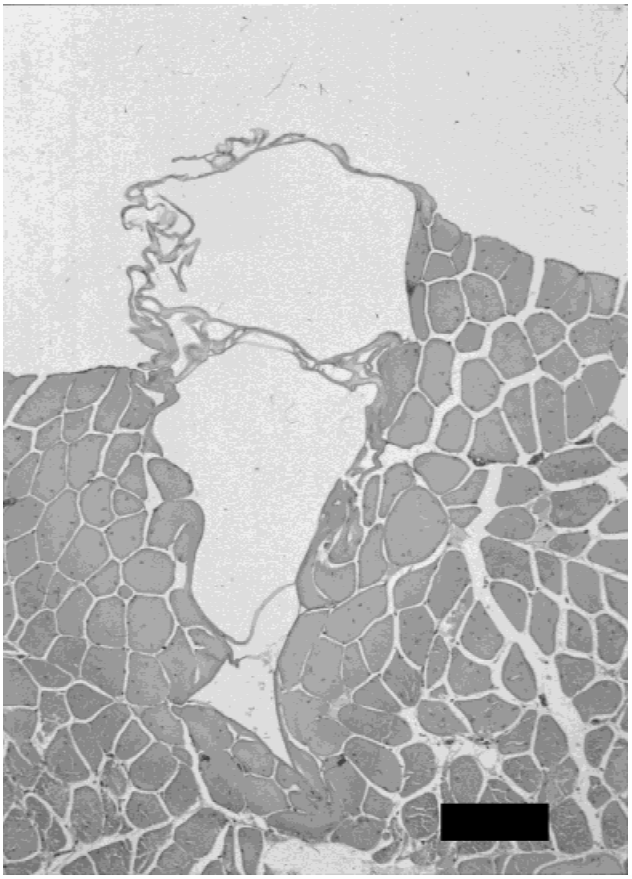

Fig. 8. Section of a slot cut in porcine tissue, under the same conditions as those used in Figure 7, after two passes across the focus of the laser beam. There is minimal damage at the margins and no sign of carbonization. Scale bar = 100 μm.

a charred boundary layer. Although the appearance of well-defined, normal muscle tissue at hole and slot edges is encouraging for the prospects of tissue regrowth, in vivo studies are required to evaluate long-term healing success.

CONCLUSIONS

The first studies of the interaction between a 2-μm Tm-doped silica fiber laser and biological tissue have been presented. The laser–tissue interaction has been shown to be similar in nature to other cw interactions but at the same time exhibits characteristics of photothermal ablation processes, typical of strongly absorbed lasers operating in the mid-infrared region. The rapid ablation rate and the ability to form well-defined lesions with minimal damage at boundaries have demonstrated the potential of this fiber laser to fulfil applications in the medical field. Our future studies will address the suitability of this and other fiber laser sources for specific medical applications.

ACKNOWLEDGMENTS

We gratefully acknowledge the assistance of Professor Philip Sloan and Sue Holland of the University Dental Hospital of Manchester in processing and interpreting the histology.

REFERENCES

1. Hale GM, Querry MR. Optical constants of water in the 200-nm to 200-μm wavelength region. Appl Opt 1973;12: 555–563.
2. Verdaasdonk RM, van Swol CFP. Laser light delivery systems for medical applications. Phys Med Biol 1997;42: 869–894.
3. Azzolini C, Gobbi PG, Brancato R, Trabucchi G, Codenotti M. New semiconductor laser for vitreoretinal surgery. Lasers Surg Med 1996;19:177–183.
4. Muendel M, Engstrom B, Kea D, Laliberte B, Minns R, Robinson R, Rockney B, Zhang Y, Collins R, Gavrilovic P, Rowley A. 35-Watt cw single mode ytterbium fiber laser at 1.1 μm. In: 1997 OSA technical digest series: conference on lasers and electro-optics. Vol 11. Washington, DC: Optical Society of America, 1997; p CPD30-1.
5. Jackson SD, King TA. High-power diode-cladding-pumped Tm-doped silica fiber laser. Opt Lett 1998;23: 1462–1464.
6. LeCarpentier GL, Motamedi M, McMath LP, Rastegar S, Welch AJ. Continuous wave laser ablation of tissue: analysis of thermal and mechanical events. IEEE Trans Biomed Eng 1993;40:188–200.
7. Verdaasdonk RM, Borst C, van Gemert MJC. Explosive onset of continuous wave laser tissue ablation. Phys Med Biol 1990;35:1129–1144.
8. Youell PD, Dickinson MR, King TA. Investigations into the interaction of a high power semiconductor diode laser with biological tissue. Proc SPIE 1993;2077:109–117.
9. Pearce J, Thomsen S. Rate process analysis of thermal damage. In: Welch AJ, van Gemert MJC, editors. Optical–thermal response of laser irradiated-tissue. New York: Plenum, 1995; p 570–584.
10. Domankevitz Y, McMillan K, Nishioka NS. Characterization of tissue ablation with a continuous wave holmium laser. Lasers Surg Med 1996;19:97–102.
11. McKenzie AL. Physics of thermal processes in laser–tissue interaction. Phys Med Biol 1990;35:1175–1209.